INSTITUTE OF PHYSICS PUBLISHING PLASMA SOURCES SCIENCE AND TECHNOLOGY

Plasma Sources Sci. Technol. **14** (2005) 412–418 doi:10.1088/0963-0252/14/3/002

High stability of atmospheric pressure plasmas containing carbon tetrafluoride and sulfur hexafluoride

X Yang[1], M Moravej[1], S E Babayan[2], G R Nowling[1] and R F Hicks[1]

[1] Department of Chemical Engineering, University of California, Los Angeles, CA 90095, USA

[2] Surfx Technologies LLC, 3617 Hayden Ave., Culver City, CA 90232, USA

E-mail: rhicks@ucla.edu

Received 8 October 2004, in final form 2 February 2005
Published 10 May 2005
Online at stacks.iop.org/PSST/14/412

Abstract

The properties of electronegative discharges operating at atmospheric pressure have been investigated. The plasma source consisted of two parallel metal electrodes into which helium was fed with 0.5–8.0 Torr carbon tetrafluoride or sulfur hexafluoride. It was found that the ionization mechanism changed from the α- to the γ-mode at a critical RF power level. In pure helium, this resulted in an abrupt drop in the voltage with increasing current, whereas for the fluorine-containing plasmas, a smooth, continuous transition was observed along the I–V curve. The electron densities in the plasmas fed with 4.0 Torr CF_4 and SF_6 were calculated to be $7.0 \pm 2.0 \times 10^{11}$ cm^{-3}, or about 30 times lower than that estimated for the pure helium case. Free electrons were consumed by electron attachment to the gas molecules, which boosted the density of negative ions to $\sim 10^{13}$ cm^{-3}. Compared with pure He, the lower electron density in the fluorine-containing plasmas removed the ionization instabilities encountered in the γ-mode and made it possible to sustain these discharges over substantially larger areas.

1. Introduction

Fluorine-containing plasmas are widely used for manufacturing microelectronic devices in the semiconductor industry. Reactive ion etching (RIE) of silicon oxide and silicon nitride with fluorine atoms generated in low-pressure plasmas has been indispensable for defining the sub-micrometre features found in the very large scale integrated circuits (ICs) [1–4]. In addition, fluorine plasmas have been used to etch silicon, silicon carbide, tungsten and tungsten silicide films, as well as to clean wafers and deposit fluorocarbon films [1, 2, 5–8]. Atmospheric pressure, fluorine-containing plasmas are of interest for the isotropic etching of silicon and metal films [9, 10], and decontamination of transuranic wastes [11, 12]. Operating plasmas at atmospheric pressure does not require vacuum systems and is suitable for continuous, assembly-line manufacturing [13, 14].

Fluorine plasmas operating at low-pressure are often fed with fluoride compounds, such as CF_4, SF_6, NF_3, CHF_3 and C_2F_6. These gases are known as 'electronegative' molecules, having an electron affinity of 0.5–3.0 eV [15]. In these discharges, an unusually high density of negative ions is produced owing to fast electron attachment reactions. The existence of negative ions can alter the electron energy distribution and the sheath structure, affecting the spatial distribution of the plasma potential and by neutralization, influence the total positive ion density as well as its spatial distribution. There have been extensive experimental and theoretical studies of low-pressure, electronegative gas discharges [1, 16–25]. By contrast, far fewer studies have examined the properties of atmospheric pressure plasmas containing fluorine molecules.

We have shown that low-temperature, atmospheric pressure discharges may be produced between two closely spaced metal electrodes supplied with radio-frequency (RF) power at 13.56 MHz. This plasma operates with flowing helium or argon that contains small quantities of gas molecules, <2.0 vol% [13, 26–28]. A uniform gas discharge is produced

that is quite suitable for the downstream processing of materials, such as surface treatment, etching and thin film deposition [10, 12, 27–32].

In this paper, we describe the properties of an atmospheric pressure, RF plasma fed with carbon tetrafluoride and sulfur hexafluoride. Current, voltage and power measurements have been employed in this work. It is found that the electron density in these discharges is about one order of magnitude lower than that found in pure helium plasmas. By contrast, negative ions are present in much higher concentrations and have a stabilizing influence on the atmospheric pressure discharge.

2. Experimental methods

A schematic of the atmospheric pressure plasma used in this study is shown in figure 1. It consisted of two parallel electrodes made of aluminium. The gap spacing between the electrodes was 1.2 mm unless otherwise noted. The upper electrode was 2.5 × 2.5 cm^2 and was connected to a RF power supply (13.56 MHz). This electrode was embedded in a ceramic block 10.2 × 10.2 cm^2, which in turn was placed just upstream of an aluminium block, 10.2 × 10.2 cm^2. The lower electrode, measuring 10.2 cm wide by 20.4 cm long, was grounded and cooled with chilled water. These parts were assembled together to provide a uniform duct 1.2 mm in height throughout the length of the device. Note that an upper electrode with dimensions of 7.6 × 7.6 mm^2 was used to operate the pure helium plasma. The plasma was operated at a total flow rate of 20 litre min^{-1}, which produced a linear velocity of 10 m s^{-1}. The corresponding Reynolds number was 140. The helium was of ultra-high purity (99.999%), while the carbon tetrafluoride and sulfur hexafluoride were of semiconductor purity (99.95%).

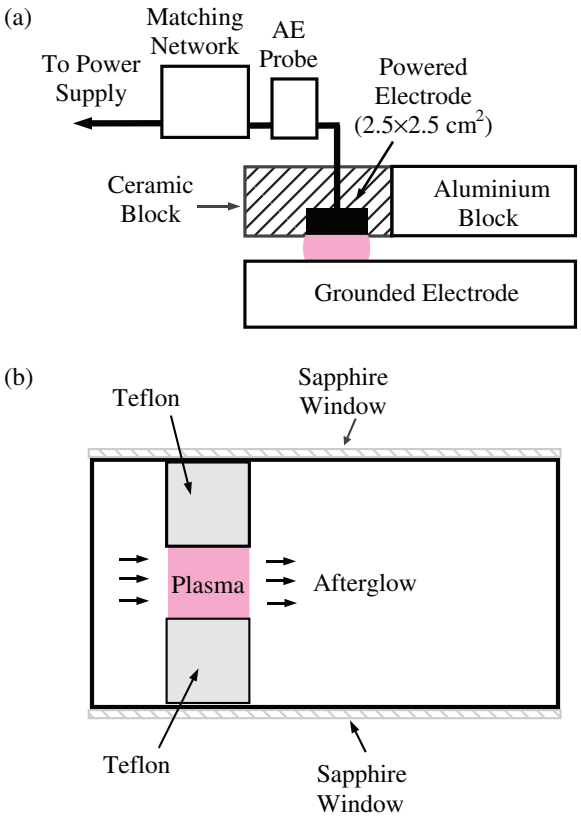

Figure 1. Schematic of the experimental apparatus: (*a*) side view, (*b*) top view.

(This figure is in colour only in the electronic version)

A tuned impedance probe (Advanced Energy RFZ 60) was inserted between the matching network and the plasma source, eliminating any cable connections, which might add inductance to the system. The plasma voltage as a function of current was determined using the Advanced Energy probe. This device yielded information on the impedance, absorbed power and phase angle between the voltage and current. It is assumed that the observed current was dominated by the conduction current through the plasma. However, the measured voltage was the sum of the potential drop through the sheaths and the bulk.

3. Results

3.1. Current–voltage relationships

Shown in figure 2 are the current–voltage (I–V) curves for the atmospheric pressure plasma fed with helium, helium and carbon tetrafluoride and helium and sulfur hexafluoride. The partial pressures of CF_4 and SF_6 were each 4.0 Torr. For pure helium, a discharge is struck at 121 V and 0.46 A (point A on the I–V curve). The discharge fills the entire gas volume and exhibits a layered structure in the direction perpendicular to the electrodes. Adjacent to the metal surfaces and at the centre of the gap the plasma is relatively dim, whereas a bright region exists 0.25 mm away from the boundaries. The discharge voltage increases linearly with the current with increasing input power. It has been shown that this abnormal glow regime is an α-mode discharge in which the plasma is sustained by bulk ionization [33, 34].

Upon increasing the power further, an abrupt transition occurs from points B to C. Here, the voltage drops from 220 to 136 V, the current increases from 0.83 to 1.2 A and the power surges from 16 to 135 W. In the meantime, the discharge shrinks to a cylindrical column and takes on a barbell shape. Bright circular discs about 5 mm in diameter

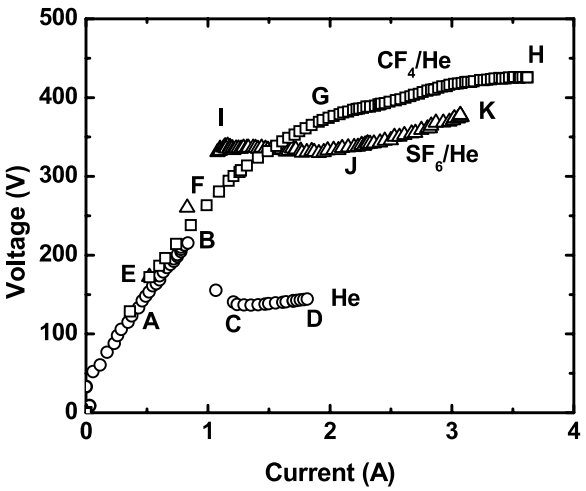

Figure 2. I–V curves for atmospheric pressure plasmas fed with pure He (○), He and 4.0 Torr CF_4 (□) and He and 4.0 Torr SF_6 (△).

are centred at the electrode surfaces, and these discs are connected by a dimmer column of light. With the input power raised from points C to D, the discharge voltage stays constant at about 140 V. In this process, the discharge becomes brighter, but its size and shape remain unchanged. We have shown that the abrupt transition in the plasma operation is due to the breakdown of the α-mode sheath and the formation of a γ-mode discharge, where the plasma is sustained by the secondary electron emission from the electrode surfaces [33, 34].

With the addition of 4.0 Torr of CF_4 to the helium plasma, the discharge ignites at 166 V and 0.49 A (point E). The discharge fills the entire space between the two electrodes and takes on a layered structure similar to that observed in the helium α-mode discharge. The voltage increases linearly with the current with increasing input power up to point F. Beyond point F, the rate of voltage increase trails off. In the meantime, it is observed that inside the discharge, bright spots form at the electrode surfaces, and randomly move about the surface. The bright spots soon merge with each other, so that the plasma enters a new operating regime at 400 V and 2.0 A (point G). This discharge has the characteristics of a γ-mode discharge in which bright layers centred at the electrode surfaces are connected by a dimmer column across the gap. However, unlike the abrupt transition occurring in the helium plasma, the α- and γ-modes coexist in the CF_4 and He plasma and transition smoothly from one to the other with increasing input power. Note that the plasma is turned off at 425 V and 3.6 A (point H) when an arc appears.

In the case of adding 4.0 Torr SF_6 to the helium, the plasma ignites at 335 V and 1.1 A (point I). Here the plasma appears as a columnar discharge with bright discs located at the electrode surfaces, indicating that it operates in the γ-mode with electron generation at the surfaces dominating. The columnar discharge, often appearing at a corner of the electrode, spreads over a larger area with increasing input power. In this process, the discharge voltage remains constant at 340 V until the current reaches 2.2 A, where the plasma covers the entire surface of both electrodes (point J). The γ discharge is stable, and no arcing is observed even when the input power reaches the limit of the power supply (i.e. 1100 W, point K).

Current–voltage curves at different partial pressures of carbon tetrafluoride have been recorded and are plotted in figure 3. The gas initially breaks down at 136 V, 154 V and 166 V when containing 0.5 Torr, 2.0 Torr and 4.0 Torr of CF_4, respectively. The curves follow the same trend up to point A, where the discharge begins the transition from the α-mode to the γ-mode. For 0.5 Torr CF_4 in He, this transition is abrupt and produces a kink in the curve. By contrast, for 2.0 and 4.0 Torr CF_4 in He, the transition occurs smoothly.

Shown in figure 4 are I–V curves for atmospheric pressure plasmas fed with 0.5 Torr, 2.0 Torr, 4.0 Torr and 8.0 Torr of SF_6 in He. A Townsend dark regime is recorded until the discharges ignite at 234 V, 289 V, 335 V and 367 V, respectively. The plasma initially formed in each case exhibits a narrow glowing column with the most intense emission focused at the electrode surfaces. This indicates that the discharge operates in the γ-mode, with ionization occurring primarily by secondary electron emission. With increasing input power the columnar discharge expands and eventually occupies the entire space between the two electrodes. The dashed line through the I–V curves indicates the point where each plasma fills the gas volume. When the gas contains 8.0 Torr SF_6, the discharge is unstable upon breakdown but exhibits a steady γ-mode structure at higher powers. In no case was arcing observed. All the I–V curves terminate at 1100 W, the maximum value permitted by the power supply.

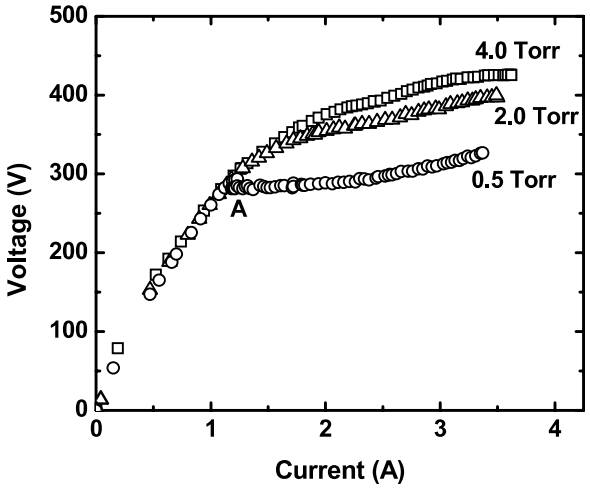

Figure 3. I–V curves of the atmospheric pressure plasma fed with different partial pressures of carbon tetrafluoride in helium.

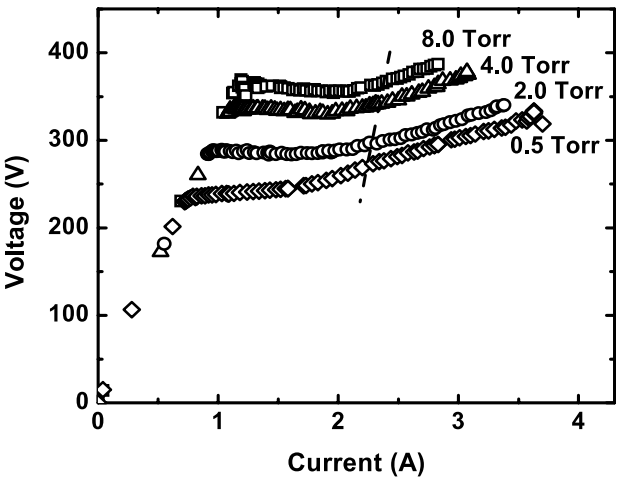

Figure 4. I–V curves of the atmospheric pressure plasma fed with different partial pressures of sulfur hexafluoride in helium.

Presented in figure 5 are the I–V curves for the sulfur hexafluoride and helium plasma at three different gap spacings, 0.8, 1.2 and 1.6 mm. One can see that the discharge voltage is higher for wider gap spacing at a given current. Following breakdown, the I–V curves are for the most part parallel to one another. Increasing the gap from 0.8 to 1.2 mm and from 1.2 mm to 1.6 mm raises the plasma voltage by an average of 40 V and 70 V, respectively.

3.2. Current–power and current–phase angle relationships

Shown in figure 6 is the dependence of the absorbed power on the current for the carbon tetrafluoride, sulfur hexafluoride

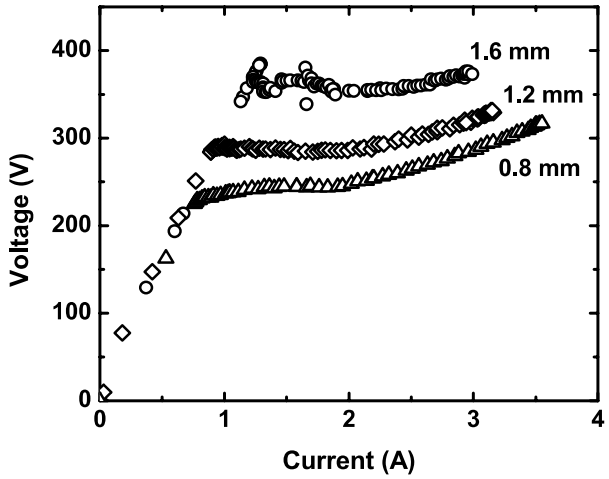

Figure 5. I–V curves as functions of gap spacing in the helium and sulfur hexafluoride plasma. The partial pressure of SF_6 is 3.0 Torr.

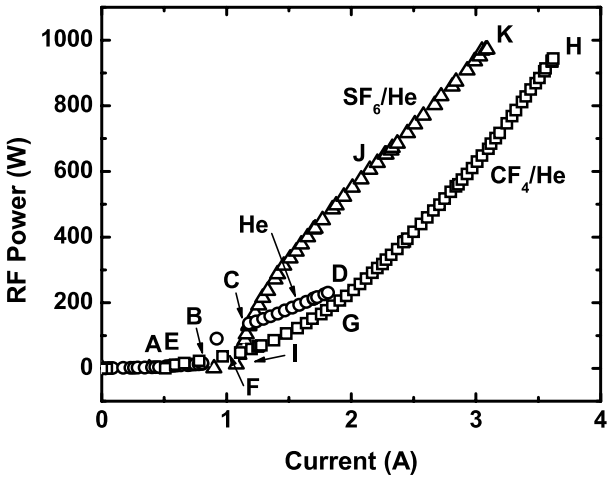

Figure 6. The dependence of the absorbed power on the discharge current in atmospheric pressure plasmas fed with pure He (○), He and 4.0 Torr CF_4 (□) and He and 4.0 Torr SF_6 (△).

and helium plasmas. The partial pressures of CF_4 and SF_6 in helium were each 4.0 Torr. The points labelled alphabetically on the graphs correspond to the same operating conditions as those indicated on the I–V curves in figure 2. The pure helium plasma ignites at a current of 0.46 A (point A), and an abrupt increase of plasma power from 16 to 135 W occurs as the discharge transforms from the α-mode to the γ-mode at points B to C. The absorbed power keeps increasing with the current after entering the γ operating mode until the plasma is turned off at 232 W and 1.8 A (point D). Here, the power density is 9.8 kW cm^{-3}.

The α-mode CF_4 and He plasma is struck at point E. The maximum power absorbed in this discharge is 40 W at point F, corresponding to a power density of 52 W cm^{-3}. Beyond point F, the γ-mode gradually takes over, replacing the α-mode completely at 200 W and 2.0 A (point G). Thereafter, the slope of the P–V curve increases with the applied power until a maximum value of 948 W and 3.6 A is reached (point H). Here, the power density equals 1.2 kW cm^{-3}, which is a 20-fold increase over the highest value attained in the α-mode (point F).

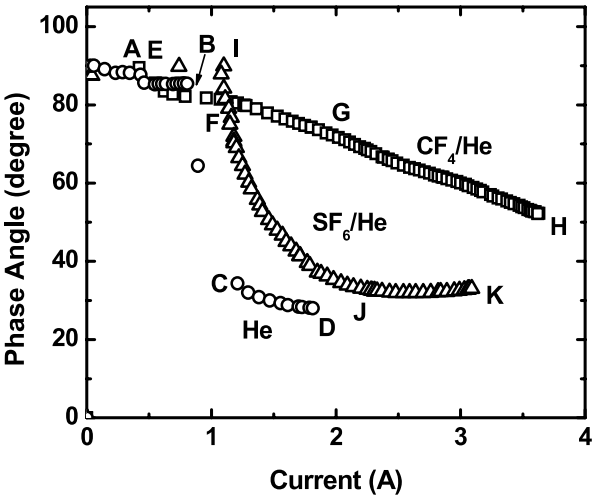

Figure 7. The dependence of the voltage–current phase angle on the discharge current in atmospheric pressure plasmas fed with pure He (○), He and 4.0 Torr CF_4 (□) and He and 4.0 Torr SF_6 (△).

With 4.0 Torr SF_6 in He, the columnar discharge ignites at 1.1 A (point I) and spreads with increasing power until the entire space between the two electrodes is filled at 615 W and 2.2 A (point J). Beyond this point, the P–V curve is parallel to that recorded for the CF_4 and He plasma. It is noted that at the same current, the power absorbed in the SF_6 plasma is about 350 W higher than in the CF_4 plasma. The discharge is turned off at 970 W and 3.1 A (point K), where the power density reaches a maximum value of 1.2 kW cm^{-3}.

Presented in figure 7 is the dependence of the phase angle (between the voltage and current) on the current for the CF_4, SF_6 and He plasmas. The alphabetically labelled points on these curves correspond to the same operating conditions as those indicated in figures 2 and 6. For pure helium, the gas breaks down at point A, and after that the phase angle remains constant at about 85.0° before the α-to-γ transition occurs at point B. This confirms that the α-mode is a capacitive discharge. From points B to C, the phase angle falls from 85.0° to 31.0° as the plasma transforms into the γ-mode and becomes more resistive. In the case of the CF_4 and He plasma, the phase angle begins decreasing linearly at point F, where the discharge starts to switch over from the α- to the γ-mode. The phase angle drops from 81.6° at point F to 52.3° at point H. The phase angle for the SF_6 and He plasma falls rapidly from breakdown at point I to 33.0° at point J. As discussed above, point J corresponds to the condition where the discharge covers the entire surface of both electrodes. Further increasing the power from points J to K does not lead to any change in phase angle.

4. Discussion

We have investigated the operation of an atmospheric pressure, RF plasma fed with helium and small amounts of electronegative gases, CF_4 and SF_6. For pure helium, as the plasma enters the high-power γ-mode, it undergoes an abrupt change in voltage, current, power and phase angle. The plasma contracts to a small spot, and it cannot be spread out over an electrode area larger than about 5 mm in diameter.

However, with the addition of CF_4 or SF_6 to the He, the γ-mode discharge forms without any contraction in size and may be operated over an area equal to $2.5 \times 2.5\ cm^2$. Evidently, the electronegative molecules provide enhanced stability to the high-power γ discharge at atmospheric pressure.

It has been shown that in atmospheric pressure plasmas, the transition from the α- to γ-mode is due to sheath breakdown [33, 38]. However, whether or not the I–V curve changes discontinuously at this point depends on the relative thickness of the two sheaths [34]. If the α sheath is thicker than the γ sheath, the transition occurs abruptly with the discharge contracting in size, whereas if the reverse is true, then the transition will be smooth with no discharge shrinkage.

The sheath thickness, d_s, may be calculated using the following equation [1, 36]:

$$J = 1.68\varepsilon_o \left(\frac{2e\lambda_i}{M}\right)^{1/2} \frac{V_s^{3/2}}{d_s^{5/2}}, \tag{1}$$

where ε_o is the permittivity of vacuum ($F\,m^{-1}$), e is a unit of charge (C), M is the molecular weight of positive ions ($kg\,mol^{-1}$), λ_i is the mean free path of ions (m), V_s is the sheath voltage (V) and J is the conduction current density ($A\,m^{-2}$). Note that the dominant positive ions are He_2^+, CF_3^+ and SF_5^+ in the atmospheric pressure plasmas examined herein [16, 17, 22, 31, 37]. The sheath voltage was initially assumed to be equal to the plasma voltage. Then this value was corrected by recalculating the sheath voltage from equation (3) later.

For the pure helium plasma, the sheath is 77 and 15 μm thick in the α-mode and the γ-mode at points B and C on the I–V curve. Since the α sheath (B) is much thicker than the γ sheath (C), an abrupt transition occurs with a sudden drop in plasma volume. With 4.0 Torr CF_4 in the He plasma, the α and γ sheaths are 54 and 52 μm thick at points F and G on the I–V curve. In this system, the α- and γ-modes coexist, and a smooth transition occurs between these modes with increasing applied power.

We have found that for SF_6 in helium, the plasma enters the γ operating mode directly upon gas breakdown. The sheath is 40 μm at point J on the I–V curve, where the discharge fills the entire volume between the electrodes. The sheath thickness remains constant at about this value with increasing input power. The γ sheath observed in the SF_6 plasma is thinner than the corresponding γ sheath in the CF_4 plasma. This may be attributed to the higher density of charged species in the SF_6 and He discharge, which will be discussed further below.

The electron density, n_e, of the atmospheric pressure plasmas is calculated from the following equation:

$$J = -en_e\mu_e E, \tag{2}$$

where μ_e is the electron mobility ($V\,m^{-1}s^{-1}$) and E is the bulk electric field ($V\,m^{-1}$). It is assumed that the displacement current is small compared with the electron conduction current in the bulk. The bulk electric field may be calculated from the plasma voltage after subtracting the sheath voltage. The sheath voltage may be estimated from:

$$V_s = \frac{I}{2\pi f C} = \frac{I}{2\pi f}\left(\frac{d_s}{1.52\varepsilon_o A}\right), \tag{3}$$

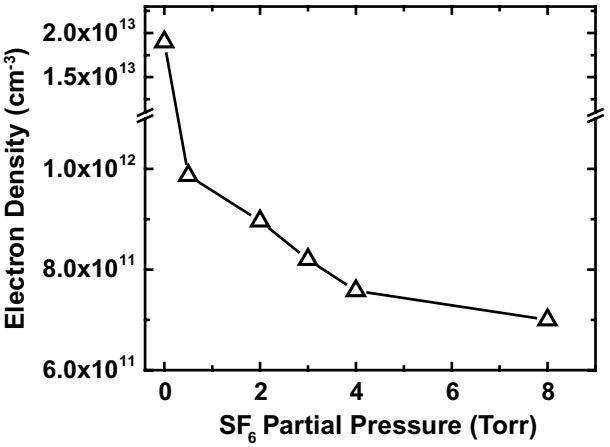

Figure 8. Electron density as a function of the SF_6 partial pressure in the atmospheric pressure plasma.

where I is the measured current (A), f is the frequency of the RF power, C is the sheath capacitance (F) and A is the discharge area (m^2).

The validity of the calculations was checked for three gap spacings of the SF_6 plasma (cf, figure 5). The bulk electric field should be relatively insensitive to the gap width [26, 39]. At a current of 3 A, the bulk electric field calculated for gaps of 0.8, 1.2 and 1.6 mm averaged $190\,kV\,m^{-1}$ with a standard deviation of $45\,kV\,m^{-1}$. This yields an uncertainty of $\pm 25\%$ in the estimated value of the electron density, which is acceptable for the purposes of this work.

Shown in figure 8 is the dependence of the electron density on the SF_6 partial pressure in the atmospheric pressure helium plasma. The plasma density decreases sharply with increasing SF_6 partial pressure. With the addition of 0.5 Torr SF_6, n_e falls from 2.0×10^{13} to $1.0 \times 10^{12}\,cm^{-3}$. Further increasing the SF_6 pressure to 8.0 Torr causes the electron density to decline gradually to $7.0 \pm 2.0 \times 10^{11}\,cm^{-3}$. A similar drop in the electron density is observed when CF_4 is added to the helium plasma.

The trend observed in figure 8 is most likely due to the high rate of electron attachment to carbon tetrafluoride and sulfur hexafluoride [15, 17, 21, 24]. The main electron attachment reactions are [16, 17, 31]

$$e + CF_4 \rightarrow CF_3 + F^- \qquad k_a \sim 5 \times 10^{-12}\,cm^3\,s^{-1}, \tag{4}$$

$$e + CF_4 \rightarrow CF_3^- + F \qquad k_a \sim 5 \times 10^{-12}\,cm^3\,s^{-1}, \tag{5}$$

$$e + SF_6 \rightarrow SF_6^- \qquad k_a \sim 10^{-9}\,cm^3\,s^{-1}, \tag{6}$$

$$e + SF_6 \rightarrow SF_5^- + F \qquad k_a \sim 10^{-9}\,cm^3\,s^{-1}. \tag{7}$$

Electrons are rapidly consumed by these processes. Attachment also impedes breakdown, and so higher voltages are required to strike the discharges, as seen in figures 2–4. Note that a decrease in the electron density by more than one order of magnitude has been observed in low-pressure helium and argon plasmas when CF_4, SF_6 or NF_3 is added to the gas [24].

Electron attachment reactions in electronegative plasmas can produce large quantities of negative ions. The existence of negative ions has a significant effect on the spatial distribution of charged particles as well as the structure of the sheath at the electrode boundary. The negative ion density, n_-,

may be determined from a simplified mass balance for the negative ions:

$$k_a n_e n_g = k_r n_+ n_-, \tag{8}$$

where k_a is the electron attachment rate coefficient ($cm^3\,s^{-1}$), k_r is the ion–ion recombination rate coefficient ($\sim 10^{-7}\,cm^3\,s^{-1}$), n_g is the density of the molecular gas (cm^{-3}) and n_+ is the positive ion density (cm^{-3}). Note that diffusion losses of negative ions are negligible because the sheath electric field prevents negative ions from reaching the electrodes. The positive ion density can be determined from the quasi-neutrality characteristics of the plasma,

$$n_+ = n_e + n_-. \tag{9}$$

By combining equations (8) and (9), one can calculate the negative ion density from the following equation:

$$n_- = n_e \left[\left(\frac{k_a/k_r}{n_e/n_g} + \frac{1}{4} \right)^{1/2} - \frac{1}{2} \right]. \tag{10}$$

We have shown that the atmospheric pressure γ-mode discharge produces electron densities of $7.0 \pm 2.0 \times 10^{11}\,cm^{-3}$ with 4.0 Torr of the fluorine-containing molecules added to the helium. By plugging these values into equation (10), we obtain negative ion densities of $1.2 \pm 0.3 \times 10^{12}\,cm^{-3}$ for the CF_4 plasma and $2.2 \pm 0.5 \times 10^{13}\,cm^{-3}$ for the SF_6 plasma. The n_- and n_e values obtained for the CF_4 plasma are consistent with our previous results [31]. Note that in the SF_6 discharge, n_- is nearly 30 times greater than n_e. The smaller sheath thickness observed for the SF_6 plasma (i.e. 40 μm) is most likely due to the high density of charged species. This is because the sheath thickness is determined by the need to transport the positive ion flux from the bulk to the electrode surface and to carry the discharge displacement current through the sheath.

The γ-mode discharge is sustained by secondary electron emission from the electrode surface as it is struck by a high flux of positive ions. In a pure helium plasma, electrons are the only negatively charged species present that can neutralize the positive ions. When operating in the γ-mode, the electron density in the pure He plasma is higher than $10^{13}\,cm^{-3}$. Such a high electron density may cause ionization instabilities, which may be responsible for the discharge contraction to a 5 mm wide disc [34]. By contrast, the addition of CF_4 and SF_6 to the helium plasma not only generates large quantities of negative ions necessary to balance the positive ions but also helps lower the electron density and reduce the ionization overheating. As a result, one can operate the atmospheric pressure γ-mode over a much broader area.

5. Conclusions

We have investigated the properties of atmospheric pressure, RF plasmas fed with helium, carbon tetrafluoride and sulfur hexafluoride. It has been shown that the α- and γ-modes of ionization may coexist in the CF_4 and He plasma and that the α–γ transition occurs smoothly without any discharge contraction. With the addition of SF_6 to the He gas, the plasma enters the γ-mode directly. The fast rate of electron attachment caused by the electronegative additives not only generates large quantities of negative ions with densities up to $10^{13}\,cm^{-3}$ but also lowers the electron density to $7.0 \pm 2.0 \times 10^{11}\,cm^{-3}$, a 30-fold decline relative to the pure He. This dramatically increases the stability of the atmospheric pressure plasma at high input power densities.

Acknowledgment

This research was supported by the US Department of Energy, Environmental Management Sciences Program (Grant No FG07-00ER45857).

References

[1] Lieberman M A and Lichtenberg A J 1994 *Principles of Plasma Discharges and Materials Processing* (New York: Wiley)
[2] Wolf S 1990 *Silicon Processing for the VLSI Era* vol 2 (Sunset Beach, CA: Lattice)
[3] Chen F F and Chang J P 2003 *Lecture Notes on Principles of Plasma Processing* (New York: Kluwer/Plenum)
[4] Nojiri K and Iguchi E 1995 *J. Vac. Sci. Technol.* B **13** 1451
[5] Chabert P, Cunge G, Booth J P and Perrin J 2001 *Appl. Phys. Lett.* **79** 916
[6] Bestwick T D and Oehrlein G S 1989 *J. Appl. Phys.* **66** 5034
[7] Biloiu C, Biloiu I A, Sakai Y, Suda Y and Ohta A 2004 *J. Vac. Sci. Technol.* A **22** 13
[8] Man P F, Gogoi B P and Mastrangelo C H 1997 *J. Microelectromech. Syst.* **6** 25
[9] Savastiouk S, Siniaguine O and Hammond M L 1991 *Solid State Technol.* **182** 277
[10] Tu V J, Jeong J Y, Schütze A, Babayan S E, Selwyn G S, Ding G and Hicks R F 2000 *J. Vac. Sci. Technol.* A **18** 2799
[11] Windarto H F, Matsumoto T, Akatsuka H and Suzuki M 2000 *J. Nucl. Sci. Technol.* **37** 787
[12] Yang X, Moravej M, Babayan S E, Nowling G R and Hicks R F 2004 *J. Nucl. Mater.* **324** 134
[13] Schütze A, Jeong J Y, Babayan S E, Park J, Selwyn G S and Hicks R F 1998 *IEEE Trans. Plasma Sci.* **26** 1685
[14] Kunhardt E E 2000 *IEEE Trans. Plasma Sci.* **28** 189
[15] Raizer Y P 1991 *Gas Discharge Physics* (New York: Springer)
[16] Christophorou L G, Olthoff J K and Rao M V V S 1996 *J. Phys. Chem. Ref. Data* **25** 1341
[17] Christophorou L G and Olthoff J K 2000 *J. Phys. Chem. Ref. Data* **29** 267
[18] Flamm D L and Herb G K 1989 *Plasma Etching: An Introduction* ed D M Manos and D L Flamm (New York: Academic)
[19] Winters H F and Coburn J W 1992 *Surf. Sci. Rep.* **14** 161
[20] Kline L E 1986 *IEEE Trans. Plasma Sci.* **14** 145
[21] Raul S, Ventzek P L G, Abraham I C, Hebner G A and Woodworth J R 2002 *J. Appl. Phys.* **92** 6998
[22] Bederski K and Wojcik L 1996 *Int. J. Mass Spectrom. Ion Process.* **154** 145
[23] Hebner G A and Abraham I C 2002 *J. Appl. Phys.* **91** 9539
[24] Kono A, Konish M and Kato K 2002 *Thin Solid Films* **407** 198
[25] Lichtenberg A J, Vahedi V and Lieberman M A 1994 *J. Appl. Phys.* **75** 2339
[26] Park J, Henins I, Hermann H W, Selwyn G S and Hicks R F 2001 *J. Appl. Phys.* **89** 20
[27] Nowling G R, Babayan S E, Jankovic V and Hicks R F 2002 *Plasma Sources Sci. Technol.* **11** 97
[28] Moravej M, Babayan S E, Nowling G R, Yang X and Hicks R F 2004 *Plasma Sources Sci. Technol.* **13** 8
[29] Babayan S E, Ding G and Hicks R F 2001 *Plasma Chem. Plasma Process.* **21** 505

[30] Jeong J Y, Park J, Henins I, Babayan S E, Tu V J, Selwyn G S, Ding G and Hicks R F 2000 *J. Phys. Chem.* **104** 8027
[31] Yang X, Babayan S E and Hicks R F 2003 *Plasma Sources Sci. Technol.* **12** 484
[32] Babayan S E, Jeong J Y, Schütze A, Tu V J, Moravej M, Selwyn G S and Hicks R F 2001 *Plasma Sources Sci. Technol.* **10** 573
[33] Yang X, Moravej M, Nowling G R, Babayan S E, Penelon J, Chang J P and Hicks R F 2005 *Plasma Sources Sci. Technol.* **14** 314
[34] Raizer Y P, Shneider M N and Yatsenko N A 1995 *Radio-Frequency Capacitive Discharge* (Boca Raton, FL: CRC Press)
[35] Shi J J, Deng X T, Hall R, Punnett D and Kong M G 2003 *J. Appl. Phys.* **94** 6303
[36] Lieberman M A 1989 *IEEE Trans. Plasma Sci.* **17** 338
[37] Yuan X and Raja L L 2003 *IEEE Trans. Plasma Sci.* **31** 495
[38] Shi J J, Deng X T, Hall R, Punnett J D and Kong M G 2003 *J. Appl. Phys.* **94** 6303
[39] Moravej M, Yang X, Nowling G R, Chang J P, Babayan S E and Hicks R F 2004 *J. Appl. Phys.* **96** 7011